Caveolae respond to cell stretch and contribute to stretch-induced signaling

Othon L. Gervásio, William D. Phillips, Louise Cole and David G. Allen*

School of Medical Sciences, Discipline of Physiology (F13), Bosch Institute, University of Sydney, NSW 2006, Australia

*Author for correspondence (david.allen@sydney.edu.au)

Accepted 9 June 2011
Journal of Cell Science 124, 3581–3590

doi: 10.1242/jcs.084376

Summary

Caveolae are invaginations of the plasma membrane that are formed by caveolins. Caveolar membranes are also enriched in cholesterol, glycosphingolipids and signaling enzymes such as Src kinase. Here we investigate the effect of cell stretch upon caveolar dynamics and signaling. Transfection of C2 myoblasts with caveolin-3–YFP led to the formation of caveolae-like membrane pits 50–100 nm in diameter. Glycosphingolipids became immobilized and tightly packed together within caveolin-rich regions of the plasma membrane. Fluorescence resonance energy transfer (FRET) was used to assess the degree of glycosphingolipid packing. Myoblasts were subjected to a brief (1 minute) stretch on an elastic substratum. Stretch caused a reduction in glycosphingolipid FRET, consistent with a reversible unfolding of caveolar pits in response to membrane tension. Cells expressing caveolin-3–YFP also displayed an enhanced stretch-induced activation of Src kinase, as assessed by immunofluorescence. Repeated stretches resulted in the trafficking and remodeling of caveolin-3-rich membrane domains and accelerated turnover of membrane glycosphingolipids. The stretch-induced unfolding of caveolae, activation of Src and redistribution of caveolin and glycosphingolipids might reflect mechanisms of the cellular adaptation to mechanical stresses.

Key words: Caveolae, Signaling, Stretch

Introduction

Caveolae are flask-like invaginations of the plasma membrane ranging from 40–80 nm in diameter organized by caveolins and enriched in cholesterol and sphingolipids (Engelman et al., 1998). Caveolins have been shown to bind to many proteins involved in signaling pathways, such as G-protein subunits, tyrosine kinases, nitric oxide synthase (NOS), small GTPases and growth factor receptors (Williams and Lisanti, 2004). Caveolae are immobile when inserted in the plasma membrane, but this stability is disturbed by depletion of membrane cholesterol (with methyl-β-cyclodextrin) or depolymerization of the actin cytoskeleton (with cytochalasin D) (Thomsen et al., 2002). Thus, the assembly of caveolae by caveolin depends upon interactions (direct or indirect) with cholesterol and the actin cytoskeleton.

Even though caveolae are considered highly stable domains of the plasma membrane, they can also participate in endocytosis and transcytosis under both physiological and pathological conditions. Endocytic vesicles rich in caveolin but lacking markers for endoplasmic reticulum, *trans*-Golgi, endosome or lysosome have been named caveosomes. Caveosomes participate in the transport of the simian virus 40 and other pathogens from the cell surface to the endoplasmic reticulum (Anderson et al., 1998; Pelkmans et al., 2001) and are also involved in constitutive transport of sphingolipids and glycosylphosphatidylinositol-linked proteins from the plasma membrane to the Golgi (Nichols, 2002; Puri et al., 2001).

It has been suggested that when cells are subjected to mechanical stretch, deformation of the caveolae can trigger signaling pathways. Indeed, stretch-induced signaling by Src, RhoA, Rac1, EGFR, Erk and Akt are impaired in cells when caveolae are disrupted (Bellott et al., 2005; Kawamura et al., 2003; Naruse et al., 1998; Zeidan et al., 2003; Zhang et al., 2007). Visualization of mechanical deformation of caveolae was first described using freeze-fracture and electron microscopy (Dulhunty and Franzini-Armstrong, 1975). However, caveolae are too small to resolve by light microscopy in living cells. In an attempt to investigate caveolar function in live cells, we describe a new FRET assay using confocal microscopy and cholera toxin that revealed reversible deformation of caveolae in living cells subjected to mechanical stretch. Cells expressing caveolin-3 showed enhanced Src activation in response to stretch. Furthermore, stretch induced an increase in the dynamics of caveolin-3-rich domains and accelerated the turnover of glycosphingolipids at the cell surface. The reversible unfolding of caveolae and the plasma membrane remodeling induced by mechanical stimuli might influence Src-dependent physiological and pathophysiological processes in cells.

Results

Myoblasts of the mouse line, C2, when transfected with caveolin-3–YFP revealed caveolae-like pits on their surfaces in scanning electron microscopic images (Fig. 1C,D). The average diameter of the pits in caveolin-3-transfected myoblasts used in our experiments was 60.1 nm (s.d. 29.4 nm, s.e.m. 2.7 nm, minimum of 100 caveolae in 10 myoblasts, from three independent experiments). This is consistent with previous reports (mean diameter 40–80 nm) (Engelman et al., 1998; Galbiati et al., 2000). Such invaginations of the plasma membrane were not observed in control non-transfected cells (Fig. 1A,B). At the fluorescence level, caveolin-3–YFP was concentrated in the

Journal of Cell Science

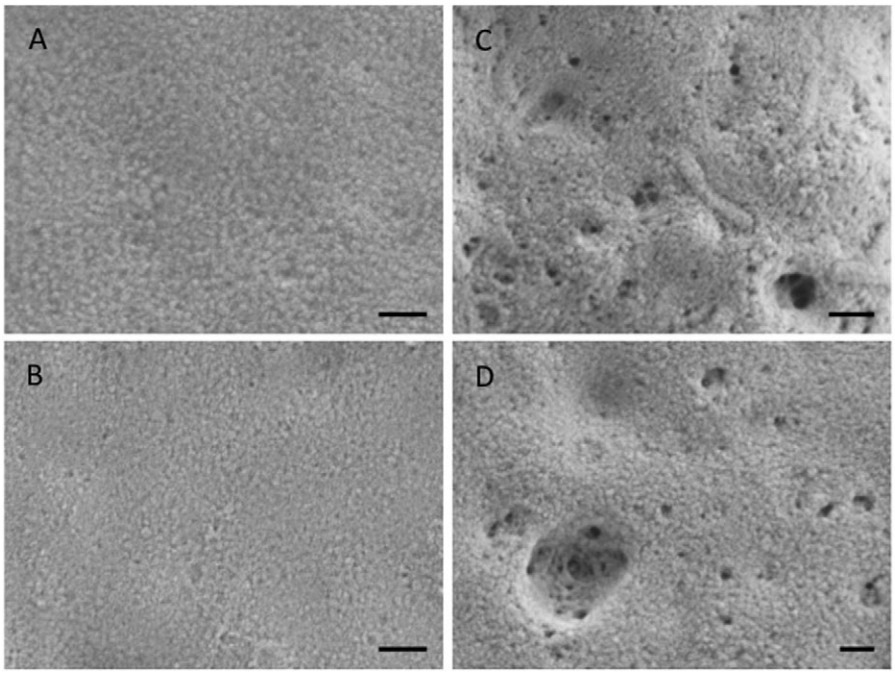

Fig. 1. Expression of caveolin-3 in C2 myoblasts induces caveolae formation. Scanning electron microscopy was used to visualize the surface of myoblasts. (**A**,**B**) Control myoblasts. (**C**,**D**) Myoblasts expressing transfected caveolin-3–YFP. The surface of the myoblasts revealed cavity-like structures (caveolae) only in dishes containing cells transfected with the caveolin-3 plasmid. Each panel shows the surface of a different cell. Scale bars: 100 nm.

plasma membrane and in intracellular compartments, as previously shown (Gervasio et al., 2008).

Caveolin-3 packs glycosphingolipids within immobile membrane domains

We used fluorescent cholera toxin to probe the effect of caveolin-3 upon the distribution of cell-surface glycosphingolipids. Myoblasts were transfected with caveolin-3–YFP for 48 hours, glycosphingolipids were tagged with cholera toxin B-subunit conjugated to Alexa Fluor 555 (1 hour, 22℃) and cells were imaged live by confocal microscopy. The lateral mobility of glycosphingolipids within the membrane was compared for caveolin-rich and caveolin-deficient membrane regions by fluorescence recovery after photobleaching (FRAP). A region of interest on the plasma membrane was chosen and the Alexa-Fluor-555-conjugated cholera toxin was selectively photobleached (Fig. 2A). Cells expressing caveolin-3–YFP on the plasma membrane showed poor recovery of fluorescence in the bleached area, indicating reduced lateral mobility of glycosphingolipids, compared with non-transfected control cells (Fig. 2A,B). We hypothesize that caveolin-3 might restrict the lateral mobility of glycosphingolipid–caveolin domains through interactions with the cytoskeleton, because caveolin binds to actin microfilaments through filamin (Stahlhut and van Deurs, 2000). Thomsen and colleagues reported that treatment of caveolin-1-expressing HeLa cells with cytochalasin D (to disrupt microfilaments) increased the mobility of surface caveolin (Thomsen et al., 2002). Indeed, treatment of C2 myoblasts expressing transfected caveolin-3–YFP with cytochalasin D restored the membrane mobility of glycosphingolipids (Fig. 2B,C). These results show that caveolin-3 can organize stable glycosphingolipid-enriched domains, presumably by interactions with microfilaments.

A Fluorescence Resonance Energy Transfer (FRET) method was used to test the influence of caveolin-3 upon the closeness of packing of glycosphingolipids. Myoblasts expressing caveolin-3–YFP were incubated with a mixture of Alexa-Fluor-555-conjugated cholera toxin (FRET donor) and Alexa-Fluor-647-conjugated cholera toxin (FRET acceptor), such that adjacent glycosphingolipid molecules would be randomly labeled with one or other of these fluorophors. Cells were then imaged using confocal microscopy and caveolin-rich and caveolin-deficient regions of interest were selected. FRET efficiency was assessed based upon the increase in the donor fluorescence after the selective photobleaching of the acceptor fluorophor. Photobleaching of the acceptor fluorophor led to an increase of the donor fluorescence both in caveolin-3-expressing and control cells, suggesting that some energy transfer occurs between adjacent cholera-toxin-labeled glycosphingolipid molecules in either situation (Fig. 3). However, the FRET efficiency was significantly greater for caveolin-3-expressing cells ($P<0.05$). The greater efficiency of FRET suggests that glycosphingolipids become more tightly packed when recruited into (submicroscopic) caveolar membrane structures (Fig. 4A).

Mechanical stretch induces reversible deformation of caveolae

Mechanical stretch has been shown to induce caveolae deformation (Dulhunty and Franzini-Armstrong, 1975). However, little is known about how resilient caveolae are when the stretch stimulus is removed and the cell returns to its original length. We therefore examined the effect of cell stretch upon glycosphingolipid packing within caveolin-rich membrane domains, as measured by FRET. Myoblasts expressing caveolin-3–YFP were cultured in stretchable silicon chambers for 48 hours and incubated with a mixture of cholera toxins as described above. The emission curve for the acceptor fluorophor (Alexa Fluor 647), when the donor was excited, was determined using single scans (Zeiss LSM 510 Meta detector; Fig. 4B,C). This spectral curve represents the energy transferred from the donor to the acceptor and provides a gauge of how close the cholera-toxin-labeled glycosphingolipids were packed within the membrane. After collecting the acceptor emission curve, cells were subjected to a 20% one-dimensional

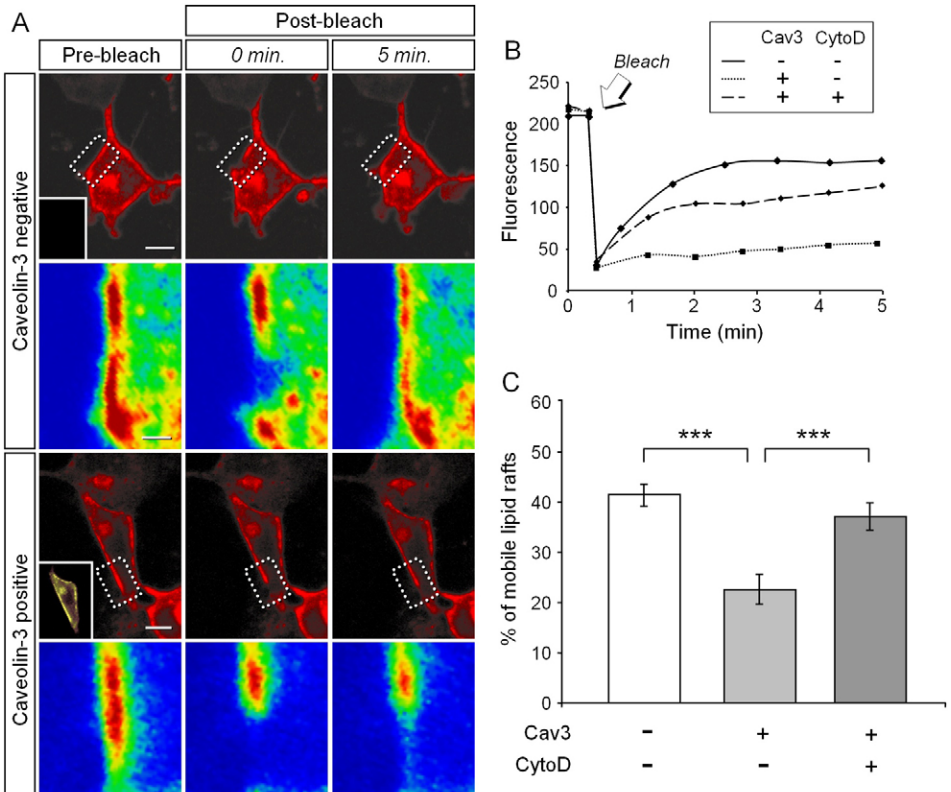

Fig. 2. Surface expression of caveolin-3 decreases the mobility of lipid rafts. The lateral mobility of Alexa-Fluor-555-conjugated cholera-toxin-labeled glycosphingolipids on the surface of C2 myoblasts assessed by FRAP. A region of interest of the plasma membrane was bleached. Recovery of the fluorescence in the bleached region was plotted against time. (**A**) Top panel shows a non-transfected cell displaying rapid recovery of fluorescence (mobile glycosphingolipid). Middle panel shows a caveolin-3–YFP-positive displaying slow recovery of fluorescence. When caveolin-positive cells were treated with cytochalasin D (bottom panel), the recovery of fluorescence was partially restored. (**B**) Quantification of fluorescence recovery over time after photobleaching in non-transfected cell and cells expressing caveolin-3, with and without cytochalasin D. (**C**) Pooled data showing that expression of caveolin-3 decreases the mobility of glycosphingolipids on the cell surface. Glycosphingolipid mobility recovered when cells are treated with cytochalasin D. Bars represents mean ± s.e.m. of minimum of six cells per group, from two independent experiments. Scale bars: 10 μm and 2 μm (inset). ***$P<0.001$.

stretch (Fig. 4B, double-headed arrow shows axis of stretch). The emission curve was again collected and compared with the one generated with the cell at resting length. Mechanical stretch induced a highly significant reduction in the FRET efficiency in caveolin-rich domains (Fig. 4C,D). No such reduction was detected in cells that did not express transfected caveolin-3. Our interpretation of this result is that the reduction in FRET efficiency represents an increase in the average spacing between cholera toxin-tagged glycosphingolipids in the caveolae, which is due to stretch-induced flattening of the caveolae (see later results).

To test the resilience of caveolae, cells were subjected to cycles of stretch followed by relaxation to the original resting length. The acceptor emission curve was collected before, during stretch and after relaxation. Fig. 4E shows two cycles of stretch–rest from a caveolae-rich membrane domain on a representative cell. During the first stretch, the caveolae domains displayed a reduced FRET efficiency, as noted above (Fig. 4A,B). When the mechanical stretch was removed, the acceptor spectral curve returned to its original shape. We then applied a second stretch stimulus, and the emission curve again showed a reduction in FRET efficiency. Following relaxation from the second stretch, the FRET efficiency once more returned to the higher resting level. These results support a model in which physiological mechanical stretch (20%) is able to cause caveolae deformation, and once this stimulus is removed, caveolae are able to return to their previous shape.

Caveolin-3 enhances Src kinase activation induced by stretch

Activation of Src by mechanical stretch has been demonstrated in several different cell types (Lodyga et al., 2002; Naruse et al., 1998; Plotkin et al., 2005). Deformation of the cytoskeleton by stretch is transmitted along actin microfilaments and actin filament associated protein (AFAP) to activate Src (Han et al., 2004). We tested the hypothesis that the expression of caveolin-3 within a cell would influence the stretch-induced activation of

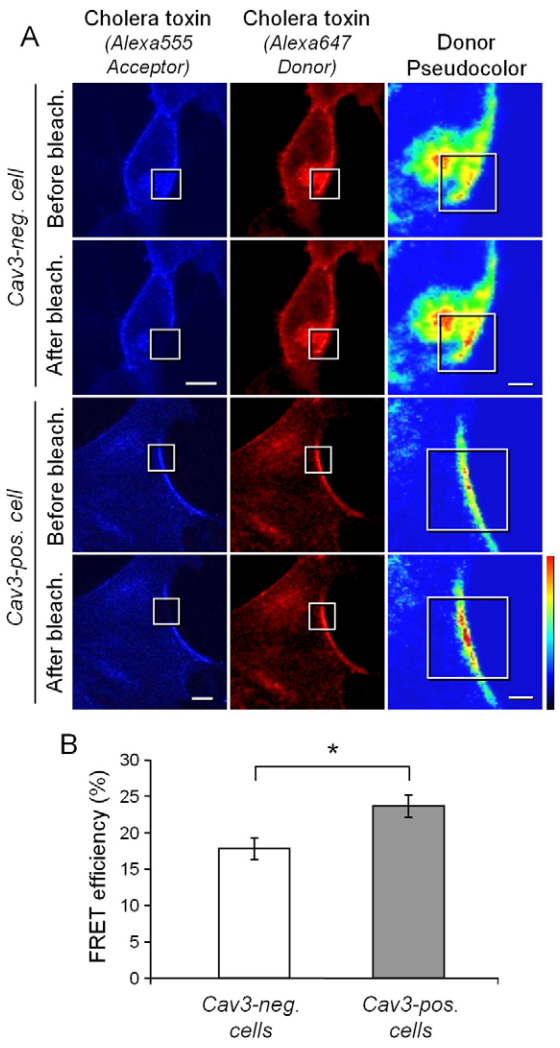

Fig. 3. Caveolin-3 expression increases packing density of lipid rafts. FRET was used to assess the degree of close packing of adjacent glycosphingolipid molecules randomly labeled with a mixture of Alexa-Fluor-555-conjugated cholera toxin and Alexa Fluor-647-conjugated cholera toxin. The FRET signal was determined by measuring the increase in donor fluorophore emission (Alexa Fluor 555) that followed photobleaching of the acceptor fluorophore (Alexa Fluor 647). FRET efficiency was greater in caveolin-3–YFP-rich membrane domains on the cell surface compared with membranes of cells lacking caveolin-3–YFP. (**A**) Top and bottom panels represent a control cell (non-transfected) and a cell expressing caveolin-3–YFP, respectively (YFP fluorescence not shown). After photobleaching of the acceptor, fluorescence in the donor channel was increased for both types of domain. (**B**) Pooled data showing higher FRET efficiency in caveolin-3–YFP-rich domains compared with controls. Bars represent mean ± s.e.m. of a minimum of ten cells per group, from three independent experiments Scale bars: 10 μm and 5 μm (inset). *P<0.05.

Src. Myoblasts were cultured on silicone chambers and transfected with caveolin-3–YFP. An acute stretch (20%) was applied to the cells and they were fixed immediately after the stimulus. Indirect immunofluorescence was performed using an antibody against the activated form of Src (phosphorylated at Tyr18). Cells were kept at stretched length during fixation, immunolabeling and imaging. Images revealed constitutively active endogenous Src kinase in both control (non-transfected) and caveolin-3–YFP-expressing C2 myoblasts (Fig. 5A). When mechanical stretch was applied, there was an increase in the mean intensity of staining for activated Src in both groups of cells. However, cells expressing caveolin-3–YFP displayed a greater stretch-induced activation of Src than was observed in non-transfected control cells (17% compared with 10%; P<0.001). Interestingly, the activated Src appeared to be concentrated in compartments deep within the cytoplasm (Fig. 5A). These results confirm previous findings that stretch is able to induce Src activation, but also show that caveolin-3 enhances the stretch-induced activation of Src kinase in myoblasts.

Stretch accelerates glycosphingolipid turnover and caveolin dynamics

It has been reported that caveolin can be translocated from caveolar to non-caveolar domains in response to hyperosmotic stress, cholesterol oxidation and depletion, heat-shock and stretch (Kang et al., 2000; Kawabe et al., 2004; Smart et al., 1994). In particular, Kawabe and colleagues reported that, following a cyclic stretch stimulus, caveolin redistributed to non-caveolar domains on the plasma membrane (Kawabe et al., 2004). This reorganization did not involve detectable internalization or intracellular trafficking of the caveolin. We first examined the effect of a single, sustained stretch upon the subcellular distribution of caveolin-3–YFP in C2 myoblasts. Cells were cultured in silicone chambers and a sustained stretch was applied for up to 90 minutes. Repeated three-dimensional image analysis was performed to assess the trafficking of caveolin during stretch. In some cells, surface clusters of caveolin-3–YFP formed when the stretch was maintained for 60 minutes or more (Fig. 6A,B, top panels). Diffuse cytoplasmic caveolin-3 was observed before the stretch and targeted to regions of the plasma membrane during the stretch stimulus. However, in some cells, pre-existing surface clusters of caveolin-3–YFP became fragmented or internalized (Fig. 6A,B, bottom panels). We could not detect any pattern of caveolin trafficking or internalization that correlated with differences in cell size, shape, cell culture density or with the level of caveolin3–YFP expression. In a third subset of cells, neither the formation of clusters nor internalization of caveolin was observed upon stretch (data not shown). Overall, stretch did not appear to favor either net assembly or disassembly of caveolin-3-rich plasma membrane domains. The effect of stretch appeared to be to increase the dynamics of caveolin-3 redistribution (incidence of assembly plus disassembly events).

This led us to investigate whether stretch might also increase the dynamics of glycosphingolipids. To do this, glycosphingolipids on the surface of living C2 myoblasts were labeled twice, before and after stretch. Myoblasts grown in silicone chambers were incubated with Alexa-Fluor-555-conjugated cholera toxin for 40 minutes at room temperature and were imaged by confocal microscopy. Cycles of stretch then rest (1 Hz) were then applied for 15 minutes, after which the cells were fixed at the original (relaxed) length. Fixed cells were incubated with Alexa-Fluor-405-conjugated cholera toxin to label any additional glycosphingolipids that had been newly inserted into the plasma membrane. Cells were reimaged and the fluorescence emissions of both Alexa Fluor 555 and Alexa Fluor 405 were measured (Fig. 7A, 'Remaining' and 'New', respectively). The intensity of residual Alexa Fluor 555 staining decreased over time in both rested and stretched groups (P<0.001), but stretched cells showed a significantly greater loss than rested cells (P<0.05; Fig 7B). By contrast, the level of newly inserted

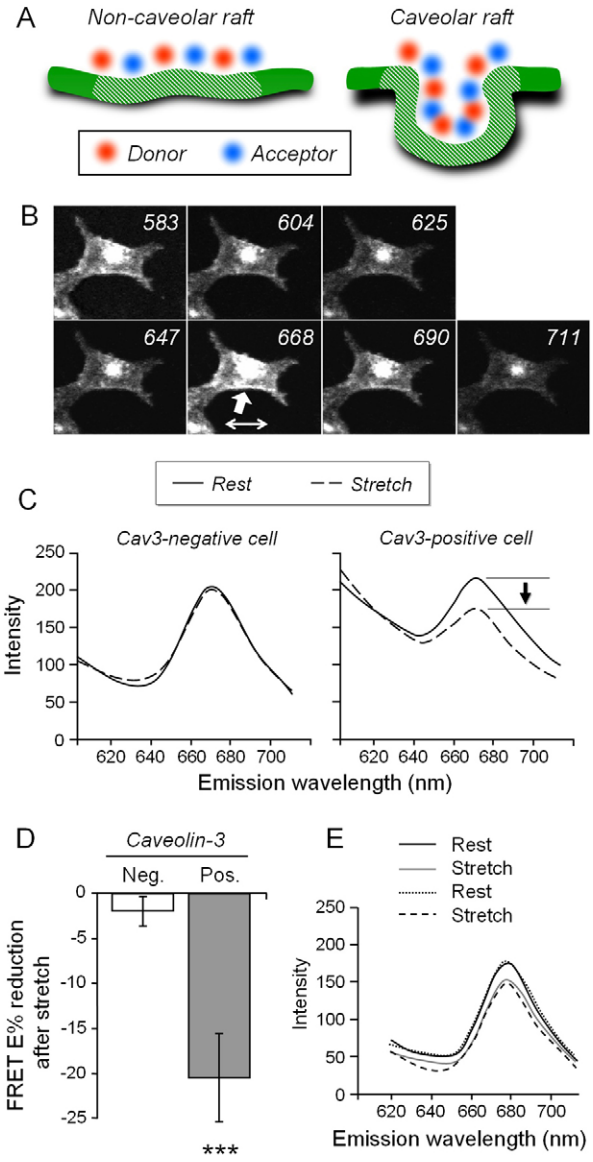

Fig. 4. Mechanical stretch induces reversible deformation of caveolae. FRET was used to compare the degree of packing of plasma membrane glycosphingolipids before and after stretch. The changes in FRET efficiency in membrane domains parallel to the axis of the stretch were determined from changes in the emission spectrum of the acceptor fluorophor. (**A**) Theoretical model of the non-caveolar and caveolar lipid microdomains. Cholera-toxin-labeled glycosphingolipids are tagged with donor fluorophor (Alexa Fluor 555, red spots) and acceptor fluorophor (Alexa Fluor 647, blue spots). (**B**) A lambda scan for each cell obtained by exciting cells with the 563 nm laser line and collecting fluorescence emissions at wavelengths ranging from 583 nm to 711 nm (note that this excludes any YFP fluorescence). The arrow in the 668 nm emission window identifies the caveolin-rich domain analyzed in C. The double arrow shows the unidirectional stretch applied to the cell. (**C**) Emission spectra for a glycosphingolipid-rich domain before and after mechanical stretch taken from a representative non-transfected control cell (Cav3-negative) and a caveolin-3-positive cell. The caveolin-3-rich domain reveals a decrease in the 668 nm acceptor emission peak, reflecting reduced FRET efficiency upon stretch. No change in the spectrum is observed in control cells. (**D**) Pooled data showing a statistically significant decrease in the FRET efficiency that occurs only for caveolin-3–YFP-positive domains. Results are means ± s.e.m. ***$P<0.001$. (**E**) Cell expressing caveolin-3 subjected to two cycles of stretch and relaxation to resting length. Spectral analysis of a representative cell shows that the emission spectrum returns to the original peak after the mechanical stretch following relaxation at the end of each cycle of stretch. Error bars in D represent mean ± s.e.m. of six cells per group, from two independent experiments.

glycosphingolipids was higher in stretched cells compared with rested control cells ($P<0.001$). The results suggest that mechanical stretch accelerated the rate of turnover of surface glycosphingolipid twofold compared with the control (turnover rate constant k for stretch, 0.02; control, 0.01; $P<0.001$).

Discussion

vCaveolin proteins have been proposed to have both structural and signaling roles at the cell surface, but their response to cell stretch remains to be fully investigated. Using a new FRET method we provide evidence that caveolae can unfold and refold in response to cell stretch. Expression of caveolin-3 potentiated the stretch-induced activation of Src kinase. Furthermore, regimes of repeated stretch accelerated the trafficking of glycosphingolipids to and from the plasma membrane, and led to remodeling of caveolin-3 membrane domains. These responses to stretch might represent mechanisms for adaptation of the cell to ongoing mechanical stresses.

Caveolae act as a dynamic mechanosensor

In first describing deformation of caveolae upon mechanical stretch, Dulhunty and Franzini-Armstrong (Dulhunty and Franzini-Armstrong, 1975) proposed that caveolae flattening might provide some of the additional membrane required to avoid rupture, when a muscle cell is stretched. Several studies have also linked the mechanical deformation of caveolae to the activation of signaling cascades (Bellott et al., 2005; Kawamura et al., 2003; Peng et al., 2008; Zhang et al., 2007). However, most evidence for the signaling role of caveolins comes from studies involving chemical methods, such as depleting cholesterol from cells. Such treatments destroy the shape of the caveolae. Confirmation of the involvement of caveolae in stretch-induced signaling also requires positive evidence that individual caveolae can reversibly deform in response to membrane stress and that caveolin expression influences downstream signaling. Here, we provide the first evidence that caveolin-3 potentiates cell signaling (Src activation) in intact cells.

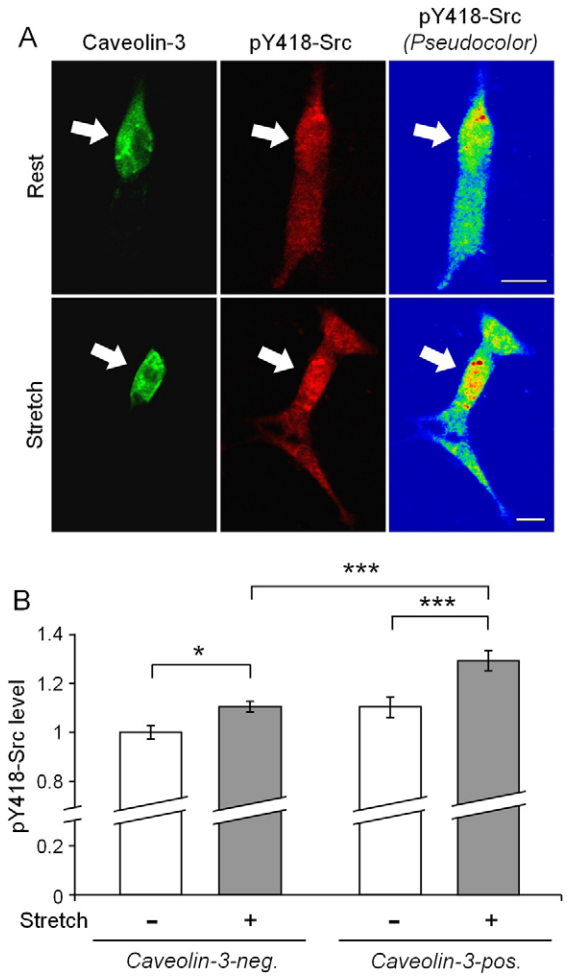

Fig. 5. Caveolin-3 enhances stretch-induced Src activation. (**A**) Myoblasts subjected to mechanical stretch for 1 minute then fixed while stretched were immunolabeled for the phosphorylated form of Src-Y418. Arrows indicate a cell that expresses caveolin-3–YFP. Scale bars: 20 μm. (**B**) Fluorescence quantification shows an increase in active Src staining in both control and caveolin-3-transfected cells following stretch. However, the degree of stretch-induced Src activation is greater in cells expressing caveolin-3, compared with non-transfected control cells. Error bars in B represent mean ± s.e.m. of a minimum of 100 cells per group, from three independent experiments. *$P<0.05$; ***$P<0.001$.

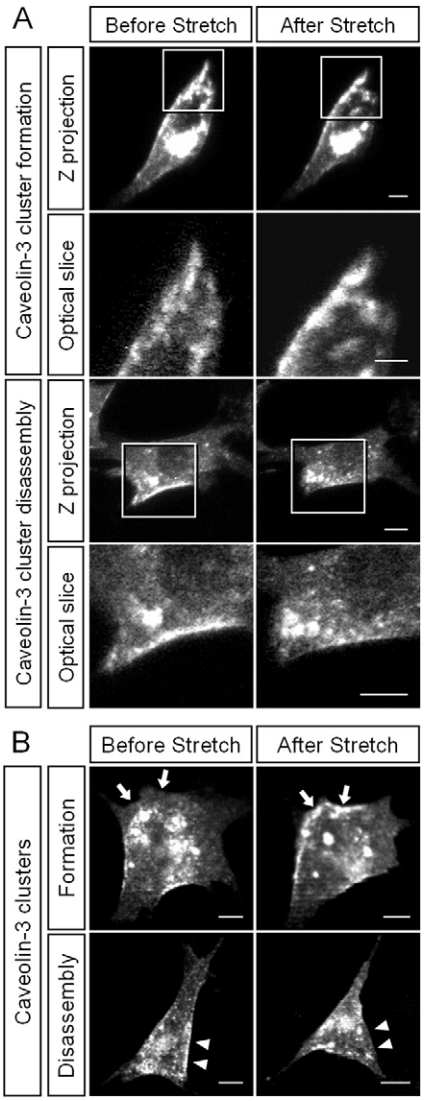

Fig. 6. Mechanical stretch promotes formation and disassembly of caveolin-3 domains. Live imaging was used to assess changes in the distribution of caveolin-3–YFP after a sustained mechanical stretch. A *Z*-stack was performed every 45 seconds for more than 90 minutes starting from before the stretch was applied. (**A**) In some cells, clusters of caveolin-3 form on the cell surface during the stretch (top two rows). However, in other cells, the pre-existing clusters of caveolin-3 become fragmented or disappeared (bottom two rows). The boxed area in each *Z*-projection is depicted at higher magnification as a single optical slice. (**B**) Optical slices of two other cells, showing formation (arrows top panel) and disassembly (arrowheads bottom panel) of caveolin-3 clusters. In each panel, the axis of stretch runs left to right. Scale bars: 10 μm.

FRET provides a means to study structural changes in caveolae in living cells. Confocal microscopy per se does not allow visualization of single caveolae or caveolar deformation, because the average size of the caveolae (~65 nm) (Parton et al., 2006) is below the limit of optical resolution (~200 nm) (Wotzlaw et al., 2007). We therefore developed a novel FRET assay to measure mechanical deformation of the plasma membrane in the low nanometer range. FRET analysis suggested that cholera-toxin-tagged glycosphingolipids were more tightly packed within membrane domains organized by caveolin-3 than in the absence of caveolae. We propose that the concave shape of the caveolae contributes to higher FRET efficiency by drawing adjacent glycosphingolipid-bound cholera toxin moieties (attached to the outer leaflet) into closer proximity (Fig. 8).

The changes in FRET efficiency suggest that caveolae reversibly flatten in response to membrane tension. Within caveolin-3–YFP-rich membrane domains, sustained stretch resulted in a significant reduction in FRET, suggesting an increase in spacing between adjacent cholera-toxin-tagged glycosphingolipids. This might be explained by an increased spacing of adjacent donor and acceptor fluorophors attached to glycosphingolipids in the flattened caveolae (Fig. 8). Furthermore, when we applied cycles of stretch and rest, the FRET efficiency from caveolin-3 membrane domains followed the stimulus dynamically. This is the first report using living cells and confocal microscopy providing evidence that caveolae are deformed by mechanical stretch and that the deformation is reversible, once the strain is removed. The spring-like ability of

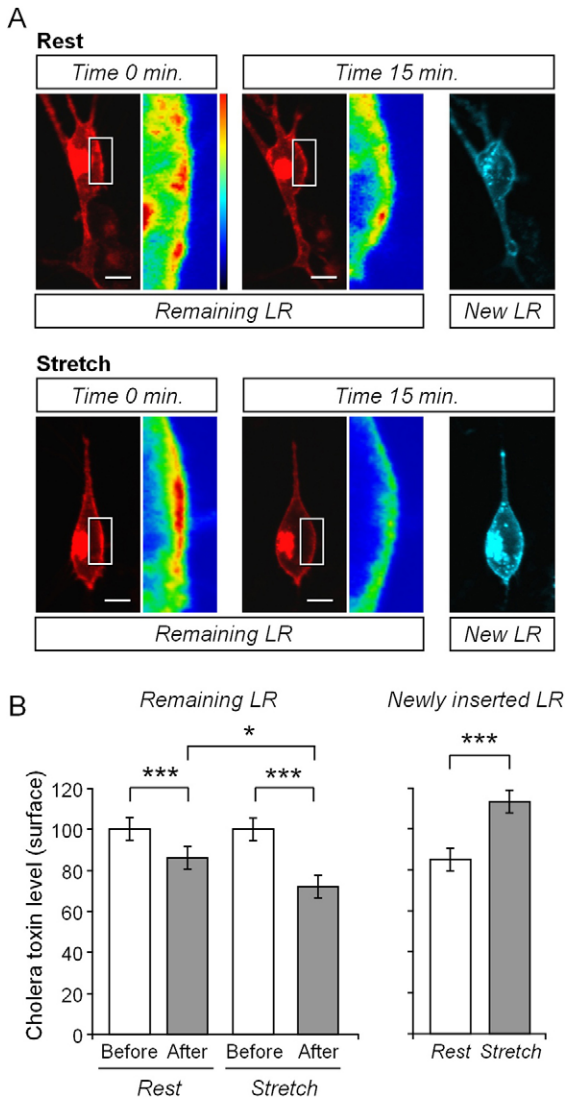

Fig. 7. Mechanical stretch accelerates the turnover of plasma membrane glycosphingolipids. Glycosphingolipids on the surface of C2 myoblasts were labeled twice to reveal changes in pre-existing and newly inserted glycosphingolipids. Pre-existing glycosphingolipids were detected with Alexa-Fluor-555-conjugated cholera toxin prior to stretch (red pseudocolor). A 'stretch and rest' (1 second stretch, 1 second rest) regime was then applied for 15 minutes followed by fixation, labeling of newly inserted glycosphingolipids with Alexa-Fluor-405-conjugated cholera toxin (blue pseudocolor) and re-imaging. (**A**) Sample cell illustrating the decline in membrane Alexa Fluor 555 labeling over time (0 minute vs 15 minutes, pseudocolor). Cells subjected to the stretch protocol show a greater loss of residual fluorescence compared to unstretched control (Remaining). When relabeled with Alexa-Fluor-405-conjugated cholera toxin after fixation, cells subjected to the stretch protocol stain more strongly for newly inserted glycosphingolipids compared with control cells (New). Scale bars: 10 μm. (**B**) Image quantification reveals the decrease in Alexa Fluor 555 fluorescence intensity remaining in membranes in both stretched and control cells. Stretched cells displayed a greater loss of residual staining than control cells (Remaining). Staining for newly inserted glycosphingolipids is greater for cells subjected to the stretch protocol (Newly inserted). Error bars represent mean ± s.e.m. of 15 cells per group, from three independent experiments. *$P<0.05$; ***$P<0.001$.

caveolae to reversibly flatten and refold, together with the known coupling of caveolins to the cytoskeleton, might help to explain the proposed role of caveolae in the transduction of stretch signaling in cells.

Src kinase activation: contributions from caveolae and cytoskeleton deformation

As mentioned previously, mechanical deformation of caveolae has been proposed to trigger a variety of signaling pathways. Src, a tyrosine kinase involved in many signaling pathways, has been reported to bind to AFAP (Lodyga et al., 2002). Cytoskeletal tension seems to be transduced into Src activation through the direct binding of AFAP to Src (Han et al., 2004). Our results indicate that stretch-induced Src activation is significantly greater in cells expressing caveolin-3. Moreover, Src activation required only a single stretch and the active Src was concentrated rather deep in the cytoplasm (Fig. 5). Stretch-evoked activation of Src might be enhanced in cells expressing caveolin-3 by several possible mechanisms. First, the unfolding of caveolae (Fig. 4) might (mechanically) amplify actin filament displacement during stretch, and thereby enhance AFAP-mediated Src activation. Second, caveolins bind to the inactive form of Src and thereby might serve as an inhibitor of Src activity at the cell periphery. It is conceivable that deformation of the caveolae releases Src from caveolin, resulting in net Src activation. A similar mechanism of activation has been proposed for RhoA and Rac1 (Kawamura et al., 2003). Further detailed experiments will be needed to test these possible mechanisms. Based on those results, we propose that the presence of caveolin-3 enhances the activation of Src kinase, but this phenomenon is likely to coexist with other endogenous mechanisms of Src kinase activation and response to stretch.

Caveolae, stretch-activated channels and calcium influx

Src family kinases can activate transient receptor potential canonical 1 channels TRPC1 (Gervasio et al., 2008), TRPC3 (Kawasaki et al., 2006) and TRPC6 (Hisatsune et al., 2004), leading to Ca^{2+} influx. The *mdx* mouse model of Duchenne muscular dystrophy involves elevated muscle expression of Src (Gervasio et al., 2008), caveolin-3 and TRPC1 (Gervasio et al., 2008; Vaghy et al., 1998; Vandebrouck et al., 2002). This pathology is also known for its altered Ca^{2+} handling and muscle cell damage triggered by influx of Ca^{2+} (Allen et al., 2005). Caveolae might therefore have a role in the pathology by producing a prolonged opening of TRPC channels through the enhanced activation of Src.

Mechanical stretch and remodeling of the plasma membrane

Cycles of stretch accelerated the turnover of glycosphingolipid from the cell surface and changes in the distribution of caveolin-3–YFP between the cell surface and intracellular pools. Cholesterol has also been shown to induce caveolin transport to the plasma membrane, and cholesterol depletion retards this process (Pol et al., 2004). Thus, shuttling of caveolin and caveolae-associated lipids are at least partially coupled. Fisher and colleagues (Fisher et al., 2004) reported that mechanical stretch was able to increase the cell surface area by insertion of lipids into the plasma membrane. Thus, accelerated redistribution of caveolin-3–YFP and turnover of glycosphingolipids might reflect a stretch-induced adaptive remodeling of the plasma membrane.

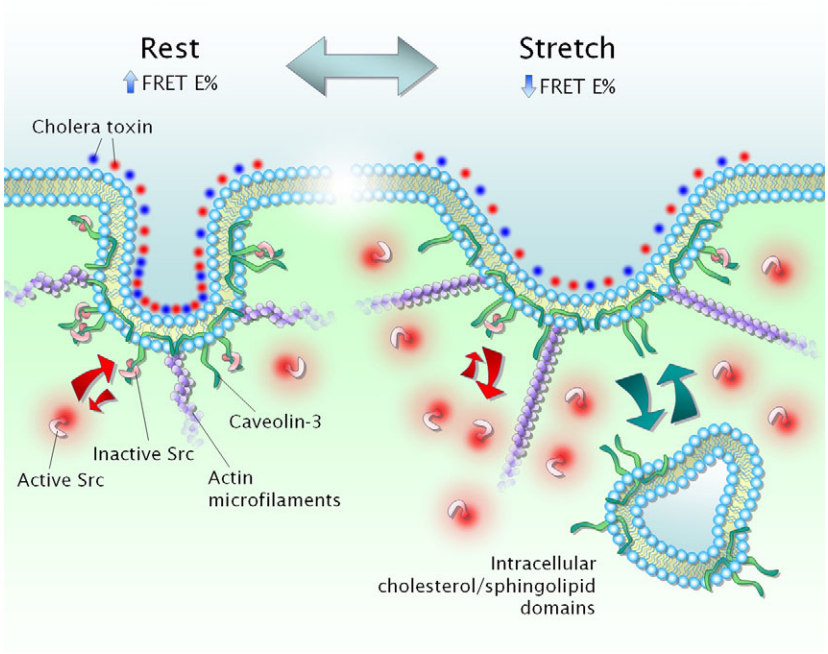

Fig. 8. Hypothetical mechanism for stretch-induced reorganization of caveolae, glycosphingolipids and Src activation. Caveolin 3 (green hairpin-like structures) forms caveolar pits in which cholera-toxin-labeled glycosphingolipids become more tightly packed (red and blue spots on outer leaflet each represent individual fluorescent cholera toxin B subunit pentamers). We propose that the elevated FRET efficiency observed in caveolin-3-positive membranes reflects tighter packing of donor and acceptor fluorophors within caveolar pits ('Rest'). The reduced FRET efficiency in stretched membranes would then reflect unfolding of caveolae ('Stretch'). It remains uncertain how caveolin-3 enhances the stretch-induced activation of Src. Stretch can act by displacement of actin filaments and AFAP, which binds directly to Src (Han et al., 2004). The presence of caveolae might increase the mechanical displacement of actin filaments during cell stretch, thereby causing greater activation of Src through AFAP. Alternatively, because interaction with caveolin can inhibit Src (Li et al., 1996), it is conceivable that conformational changes caveolin-3 during unfolding of caveolae might liberate Src, resulting in the redistribution and activation of Src kinase (red arrows). This would be similar to a mechanism proposed to activate RhoA and Rac1 (Kawamura et al., 2003). Repetitive stretch also accelerated the turnover of membrane glycosphingolipids (green arrows). These changes presumably reflect a remodeling of the plasma membrane.

Materials and Methods

Fluorescence recovery after photobleaching

FRAP experiments were carried out using a Zeiss LSM 510 Meta confocal microscope (Wetzlar, Germany) and an EC Plan-Neofluar 40× 0.75 NA water immersion objective (Zeiss). C2 myoblasts were cultured on 35 mm glass-bottom dishes (MaTek, Homer, MA) and transfected with a caveolin-3–YFP expression plasmid kindly donated by Robert Parton (Pol et al., 2004). C2 myoblasts have been used in those experiments because they do not express endogenous caveolin-3 (Song et al., 1996). Transfection was performed using Effectene reagent (Qiagen; Chatsworth, CA) according to the manufacturer's instructions. Cells were incubated with cholera toxin subunit B pentamer conjugated to Alexa Fluor 555 (2 μg/ml; Molecular Probes, Eugene, OR) for 40 minutes at room temperature (22℃) to label glycosphingolipids, and imaged by confocal microscopy. A region of interest of the plasma membrane was photobleached (563 nm laser line, 100% power, 200 iterations) and the whole cell was imaged every 5 seconds for 5 minutes at 10% laser power. The percentage of mobile lipid rafts was calculated using the Zeiss LSM 510 Meta Software version 4.2 and based on the recovery of the fluorescence level over time compared with the fluorescence before bleaching. All live-cell experiments were performed using a standard physiological solution containing 121 mM NaCl, 5 mM KCl, 1.8 mM $CaCl_2$, 0.5 mM $MgCl_2$, 0.4 mM NaH_2PO_4, 24 mM $NaHCO_3$ and 5.5 mM glucose, and equilibrated with 95% O_2, 5% CO_2.

Fluorescence resonance energy transfer

FRET was performed using a mixture of cholera toxin subunit B conjugated with either Alexa Fluor 555 or Alexa Fluor 647 (donor and acceptor: 2 μg/ml and 8 μg/ml respectively; Molecular Probes) for 45 minutes at 22℃. To maximize the energy transfer between the FRET pair, the molar ratio of the two cholera toxins was 1:4 (donor:acceptor), based on the donor geometric exclusion model (Wallrabe et al., 2003). We have previously investigated the photoconversion of Alexa Fluor 555 and Alexa Fluor 647 in unfixed material (Gervasio et al., 2007), and no photoconversion was detected using such fluorophores separately, or in combination. Cells were plated on glass-bottom dishes, transfected with caveolin-3–YFP for 48 hours, then incubated with the mixture of cholera toxins as described above. FRET efficiency was calculated using the method of acceptor photobleaching (Gervásio et al., 2007). FRET efficiency (E) was calculated from the increase of the fluorescence intensity of the donor (F) after the acceptor fluorophor was selectively photobleached (acceptor photobleached, AP) [$E=(F^{\text{After AP}}-F^{\text{Before AP}})/F^{\text{After AP}}$] (Bastiaens et al., 1996; Kenworthy, 2001).

Cells were imaged using low laser power settings (10%; 563 nm and 633 nm laser lines) and a region of interest was selectively bleached using the 633 nm laser line (100% power, ten iterations). The cells were again imaged using low laser power. FRET efficiency was calculated based on the percentage increase of the donor fluorescence after the acceptor photobleaching based on the formula above. The photobleaching of acceptor approach was used to determine differences in FRET efficiency at caveolin-3–YFP-rich and caveolin-3–YFP-deficient membrane domains.

Spectral analysis was used to determine changes in FRET efficiency (i.e. energy transfer) induced by mechanical stretch at caveolar and non-caveolar lipid rafts.

Assessment of caveolae deformation using FRET

Myoblasts were seeded in silicone chambers (Strex, Mountain View, CA) that were pretreated with gelatin (9:1 gelatin:PBS; Sigma) for 1 hour at 37℃. For the FRET experiments, cells were transfected with caveolin-3–YFP plasmid for 48 hours and incubated with a mixture of fluorescent cholera toxins as described above. Cells were subjected to a single-axis stretch (20%) using a pulse-motor-driven stretch machine (Strex). Cells were imaged by confocal microscopy (563 nm laser line, 10% power). The emission spectrum was recorded using the Meta detector (Zeiss LSM 510 Meta) between 580 nm and 711 nm. The emission curve was acquired and cells were then subjected to a 20% uni-axial stretch stimulus. For these stretch experiments, the emission spectrum was determined only for membrane domains in which the line of staining was parallel with the axis of the stretch. The spectrum curve was again acquired (stretch) and compared to the spectrum recorded in the unstretched condition.

Immunolabeling of active Src

Myoblasts cultured on silicone chambers and transfected with caveolin-3–YFP plasmid were stretched for 45 seconds (20% stretch) and immediately fixed in 2% paraformaldehyde (PFA) in PBS. Control cells were kept in the chamber with no

mechanical stimulation. After fixation, cells were permeabilized (0.5% Triton X-100, 5 minutes, 22℃) and incubated with anti-phosphorylated-Src-Tyr418 polyclonal antibody. This antibody was affinity purified such that it recognizes only the active form of Src (1:100, 1 hour 22℃; Sigma). Cells were washed in PBS twice and incubated with an anti-rabbit secondary antibody conjugated with Alexa Fluor 555 (1:500, 1 hour 22℃; Molecular Probes). Chambers were then washed twice in PBS and imaged using confocal microscopy (excitation: 563 nm laser line, 10% power; emission: band pass filter 575–610 nm).

Scanning electron microscopy

Myoblasts were cultured on glass coverslips and transfected with caveolin-3–YFP plasmid for 48 hours. Cells were fixed in 2% PFA in PBS for 15 minutes at 22℃. Transfected and control samples were mounted on a SEM stub, air-dried in a laminar flow hood and coated with gold by glow discharge (Lieske et al., 2001). Specimens were examined with a Zeiss Ultra Plus SEM at 2 kV.

Four-dimensional image acquisition

For caveolin-3 trafficking analysis, myoblasts grown on silicone chambers and transfected with caveolin-3–YFP were stretched for up to 90 minutes (20% stretch). A Z-stack of each cell was performed every 45 seconds (optical slice thickness adjusted to 1 μm). A two-dimensional image (maximum *Z*-projection) was generated for each time point. Both *Z*-projections and individual optical slices were analyzed over time to assess caveolin-3 trafficking.

For the glycosphingolipid turnover experiments, non-transfected cells were cultured on silicone chambers and incubated with Alexa-Fluor-conjugated cholera toxin (2 μg/ml) for 40 minutes at 22℃. Chambers were washed with physiological solution and cells were imaged by confocal microscopy. A series of stretch–rest cycles (1 Hz, 20% stretch) was applied to the cells for 15 minutes at 22℃. Cells were then immediately fixed in the rest position (2% PFA in PBS, 15 minutes, 22℃), washed in PBS and incubated with Alexa-Fluor-405-conjugated cholera toxin (40 minutes, 22℃). The same cells were re-imaged in both Alexa Fluor 555 and Alexa Fluor 405 channels. These fluorophores were chosen because they do not represent a FRET pair. The loss of pre-labeled lipid rafts from the cell surface was measured as a percentage drop in signal of the Alexa Fluor 555 over time. Alexa Fluor 405 fluorescence was used as an indicator of the amount of newly inserted lipid rafts in plasma membrane after the stretch cycles. Control cells were not mechanically stimulated and remained in the chamber for the same period of time as the stretch group. Calculation of the lipid raft turnover rate constant k was calculated based on the loss of Alexa Fluor 555 over time according to: $F=F_0 \exp(-kt)$, where F is the fluorescence level at any time point, F_0 the fluorescence level at 0 minutes, k the turnover rate constant and t is time (Harmel and Apell, 2006).

Statistics

Student's *t*-test (two-tailed) was used to compare means of two different groups. Analysis of variance (ANOVA) was used in situations of more than two variables (two-way ANOVA) with Tukey–Kramer post-test (Fig. 2C, Fig. 4F, Fig. 5B and Fig. 7B; GraphPad Prism 5.01, San Diego California USA). Means and s.e.m. are shown for each group.

Acknowledgements

We are grateful to Robert Parton (Institute for Molecular Bioscience, Brisbane, Australia) for kindly donating the plasmids used in this study.

Funding

We acknowledge funding from the National Health and Medical Research Council of Australia.

References

Allen, D. G., Whitehead, N. P. and Yeung, E. W. (2005). Mechanisms of stretch-induced muscle damage in normal and dystrophic muscle: role of ionic changes. *J. Physiol.* **567**, 723-735.

Anderson, H. A., Chen, Y. and Norkin, L. C. (1998). MHC class I molecules are enriched in caveolae but do not enter with simian virus 40. *J. Gen. Virol.* **79**, 1469-1477.

Bastiaens, P. I., Majoul, I. V., Verveer, P. J., Soling, H. D. and Jovin, T. M. (1996). Imaging the intracellular trafficking and state of the AB5 quaternary structure of cholera toxin. *EMBO J.* **15**, 4246-4253.

Bellott, A. C., Patel, K. C. and Burkholder, T. J. (2005). Reduction of caveolin-3 expression does not inhibit stretch-induced phosphorylation of ERK2 in skeletal muscle myotubes. *J. Appl. Physiol.* **98**, 1554-1561.

Dulhunty, A. F. and Franzini-Armstrong, C. (1975). The relative contributions of the folds and caveolae to the surface membrane of frog skeletal muscle fibres at different sarcomere lengths. *J. Physiol.* **250**, 513-539.

Engelman, J. A., Zhang, X., Galbiati, F., Volonte, D., Sotgia, F., Pestell, R. G., Minetti, C., Scherer, P. E., Okamoto, T. and Lisanti, M. P. (1998). Molecular genetics of the caveolin gene family: implications for human cancers, diabetes, Alzheimer disease, and muscular dystrophy. *Am. J. Hum. Genet.* **63**, 1578-1587.

Fisher, J. L., Levitan, I. and Margulies, S. S. (2004). Plasma membrane surface increases with tonic stretch of alveolar epithelial cells. *Am. J. Respir. Cell. Mol. Biol.* **31**, 200-208.

Galbiati, F., Volonte, D., Chu, J. B., Li, M., Fine, S. W., Fu, M., Bermudez, J., Pedemonte, M., Weidenheim, K. M., Pestell, R. G., Minetti, C., Lisanti, M. P. (2000). Transgenic overexpression of caveolin-3 in skeletal muscle fibers induces a Duchenne-like muscular dystrophy phenotype. *Proc. Natl. Acad. Sci USA* **17**, 9689-9694.

Gervásio, O. L., Armson, P. F. and Phillips, W. D. (2007). Developmental increase in the amount of rapsyn per acetylcholine receptor promotes postsynaptic receptor packing and stability. *Devl. Biol.* **305**, 262-275.

Gervasio, O. L., Whitehead, N. P., Yeung, E. W., Phillips, W. D. and Allen, D. G. (2008). TRPC1 binds to caveolin-3 and is regulated by Src kinase: role in Duchenne muscular Dystrophy. *J. Cell Sci.* **121**, 2246-2255.

Han, B., Bai, X.-H., Lodyga, M., Xu, J., Yang, B. B., Keshavjee, S., Post, M. and Liu, M. (2004). Conversion of Mechanical Force into Biochemical Signaling. *J. Biol. Chem.* **279**, 54793-54801.

Harmel, N. and Apell, H. J. (2006). Palytoxin-induced effects on partial reactions of the Na,K-ATPase. *J. Gen. Physiol.* **128**, 103-118.

Hisatsune, C., Kuroda, Y., Nakamura, K., Inoue, T., Nakamura, T., Michikawa, T., Mizutani, A. and Mikoshiba, K. (2004). Regulation of TRPC6 channel activity by tyrosine phosphorylation. *J. Biol. Chem.* **279**, 18887-18894.

Kang, Y. S., Ko, Y. G. and Seo, J. S. (2000). Caveolin internalization by heat shock or hyperosmotic shock. *Exp. Cell Res.* **255**, 221-228.

Kawabe, J., Okumura, S., Lee, M. C., Sadoshima, J. and Ishikawa, Y. (2004). Translocation of caveolin regulates stretch-induced ERK activity in vascular smooth muscle cells. *Am. J. Physiol. Heart Circ. Physiol.* **286**, H1845-H1852.

Kawamura, S., Miyamoto, S. and Brown, J. H. (2003). Initiation and transduction of stretch-induced RhoA and Rac1 activation through caveolae: cytoskeletal regulation of ERK translocation. *J. Biol. Chem.* **278**, 31111-31117.

Kawasaki, B. T., Liao, Y. and Birnbaumer, L. (2006). Role of Src in C3 transient receptor potential channel function and evidence for a heterogeneous makeup of receptor- and store-operated Ca2+ entry channels. *Proc. Natl. Acad. Sci. USA.* **103**, 335-340.

Kenworthy, A. K. (2001). Imaging protein-protein interactions using fluorescence resonance energy transfer microscopy. *Methods.* **24**, 289-296.

Li, S., Couet, J. and Lisanti, M. P. (1996). Src tyrosine kinases, Galpha subunits, and H-Ras share a common membrane-anchored scaffolding protein, caveolin. Caveolin binding negatively regulates the auto-activation of Src tyrosine kinases. *J. Biol. Chem.* **271**, 29182-29190.

Lieske, J. C., Toback, F. G. and Deganello, S. (2001). Sialic acid-containing glycoproteins on renal cells determine nucleation of calcium oxalate dihydrate crystals. *Kidney Int.* **60**, 1784-1791.

Lodyga, M., Bai, X. H., Mourgeon, E., Han, B., Keshavjee, S. and Liu, M. (2002). Molecular cloning of actin filament-associated protein: a putative adaptor in stretch-induced Src activation. *Am. J. Physiol. Lung Cell Mol. Physiol.* **283**, L265-L274.

Naruse, K., Sai, X., Yokoyama, N. and Sokabe, M. (1998). Uni-axial cyclic stretch induces c-src activation and translocation in human endothelial cells via SA channel activation. *FEBS Lett.* **441**, 111-115.

Nichols, B. J. (2002). A distinct class of endosome mediates clathrin-independent endocytosis to the Golgi complex. *Nat. Cell Biol.* **4**, 374-378.

Parton, R. G., Hanzal-Bayer, M. and Hancock, J. F. (2006). Biogenesis of caveolae: a structural model for caveolin-induced domain formation. *J. Cell Sci.* **119**, 787-796.

Pelkmans, L., Kartenbeck, J. and Helenius, A. (2001). Caveolar endocytosis of simian virus 40 reveals a new two-step vesicular-transport pathway to the ER. *Nat. Cell Biol.* **3**, 473-483.

Peng, F., Wu, D., Ingram, A. J., Zhang, B., Gao, B. and Krepinsky, J. C. (2008). RhoA activation in mesangial cells by mechanical strain depends on caveolae and caveolin-1 interaction. *J. Am. Soc. Nephrol.* **18**, 189-198.

Plotkin, L. I., Mathov, I., Aguirre, J. I., Parfitt, A. M., Manolagas, S. C. and Bellido, T. (2005). Mechanical stimulation prevents osteocyte apoptosis: requirement of integrins, Src kinases, and ERKs. *Am. J. Physiol. Cell Physiol.* **289**, C633-C643.

Pol, A., Martin, S., Fernandez, M. A., Ferguson, C., Carozzi, A., Luetterforst, R., Enrich, C. and Parton, R. G. (2004). Dynamic and regulated association of caveolin with lipid bodies: modulation of lipid body motility and function by a dominant negative mutant. *Mol. Biol. Cell.* **15**, 99-110.

Puri, V., Watanabe, R., Singh, R. D., Dominguez, M., Brown, J. C., Wheatley, C. L., Marks, D. L. and Pagano, R. E. (2001). Clathrin-dependent and -independent internalization of plasma membrane sphingolipids initiates two Golgi targeting pathways. *J. Cell Biol.* **154**, 535-547.

Smart, E. J., Ying, Y. S., Conrad, P. A. and Anderson, R. G. (1994). Caveolin moves from caveolae to the Golgi apparatus in response to cholesterol oxidation. *J. Cell. Biol.* **127**, 1185-1197.

Song, K. S., Scherer, P. E., Tang, Z., Okamoto, T., Li, S., Chafel, M., Chu, C., Kohtz, D. S. and Lisanti, M. P. (1996). Expression of caveolin-3 in skeletal, cardiac, and smooth muscle cells. Caveolin-3 is a component of the sarcolemma and co-fractionates with dystrophin and dystrophin-associated glycoproteins. *J. Biol. Chem.* **271**, 15160-15165.

Stahlhut, M. and van Deurs, B. (2000). Identification of filamin as a novel ligand for caveolin-1, evidence for the organization of caveolin-1-associated membrane domains by the actin cytoskeleton. *Mol. Biol. Cell.* **11**, 325-337.

Thomsen, P., Roepstorff, K., Stahlhut, M. and van Deurs, B. (2002). Caveolae are highly immobile plasma membrane microdomains, which are not involved in constitutive endocytic trafficking. *Mol. Biol. Cell.* **13**, 238-250.

Vaghy, P. L., Fang, J., Wu, W. and Vaghy, L. P. (1998). Increased caveolin-3 levels in mdx mouse muscles. *FEBS Lett.* **431**, 125-127.

Vandebrouck, C., Martin, D., Colson-Van Schoor, M., Debaix, H. and Gailly, P. (2002). Involvement of TRPC in the abnormal calcium influx observed in dystrophic (mdx) mouse skeletal muscle fibers. *J. Cell Biol.* **158**, 1089-1096.

Wallrabe, H., Elangovan, M., Burchard, A., Periasamy, A. and Barroso, M. (2003). Confocal FRET microscopy to measure clustering of ligand-receptor complexes in endocytic membranes. *Biophys. J.* **85**, 559-571.

Williams, T. M. and Lisanti, M. P. (2004). The Caveolin genes: from cell biology to medicine. *Ann. Med.* **36**, 584-595.

Wotzlaw, C., Otto, T., Berchner-Pfannschmidt, U., Metzen, E., Acker, H. and Fandrey, J. (2007). Optical analysis of the HIF-1 complex in living cells by FRET and FRAP. *FASEB J.* **21**, 700-707.

Zeidan, A., Broman, J., Hellstrand, P. and Swärd, K. (2003). Cholesterol dependence of vascular ERK1/2 activation and growth in response to stretch: role of endothelin-1. *Arterioscler. Thromb. Vasc. Biol.* **23**, 1528-1534.

Zhang, B., Peng, F., Wu, D., Ingram, A. J., Gao, B. and Krepinsky, J. C. (2007). Caveolin-1 phosphorylation is required for stretch-induced EGFR and Akt activation in mesangial cells. *Cell Signal.* **19**, 1690-1700.